

# Compression of the Choroid by Horizontal Duction

Jessica Y. Chen,<sup>1</sup> Alan Le,<sup>2-4</sup> Lindsay M. De Andrade,<sup>2,4</sup> Toshiaki Goseki,<sup>2,4</sup> and Joseph L. Demer<sup>2-6</sup>

<sup>1</sup>Computational and Systems Biology Interdepartmental Program, University of California, Los Angeles, Los Angeles, California, United States

<sup>2</sup>Department of Ophthalmology, University of California, Los Angeles, Los Angeles, California, United States

<sup>3</sup>Bioengineering Interdepartmental Program, University of California, Los Angeles, Los Angeles, California, United States

<sup>4</sup>Stein Eye Institute, University of California, Los Angeles, Los Angeles, California, United States

<sup>5</sup>Department of Neurology, University of California, Los Angeles, Los Angeles, California, United States

<sup>6</sup>David Geffen Medical School, University of California, Los Angeles, Los Angeles, California, United States

Correspondence: Joseph L. Demer, Stein Eye Institute, 100 Stein Plaza, UCLA, Los Angeles, CA 90095-7002, USA; email: jld@jsei.ucla.edu.

Submitted: May 14, 2019

Accepted: September 18, 2019

Citation: Chen JY, Le A, De Andrade LM, Goseki T, Demer JL. Compression of the choroid by horizontal duction. *Invest Ophthalmol Vis Sci*. 2019;60:4285-4291. <https://doi.org/10.1167/iovs.19-27522>

**PURPOSE.** The optic nerve becomes tethered in adduction in most people, which deforms the disc. We investigated the effect of horizontal ocular duction and subject age on choroidal volume at the macular side of the optic disc.

**METHODS.** In 25 younger (18-33 years) and 15 older (50-73 years) normal subjects, the disc and the peripapillary choroid were imaged with optical coherence tomography (OCT) in central gaze and 35° adduction and abduction. The choroid temporal to the optic disc underlying the region between the Bruch's membrane opening and fovea was segmented into regions that were multiples of the disc radius for determination of local choroidal thickness. Regional volume changes from central gaze were determined in adduction and abduction.

**RESULTS.** In adduction, regional choroidal volume decreased by  $42.4 \pm 3.4$  nanoliters (nL) (standard error of the mean) in younger ( $P < 0.0001$ ) and  $6.2 \pm 2.6$  nL in older ( $P < 0.02$ ) subjects. Relative volume reduction in adduction was  $7.5\% \pm 0.6\%$  in younger ( $P < 0.001$ ) and  $1.3\% \pm 0.6\%$  in older ( $P < 0.02$ ) subjects. Volume reduction was greatest near the disc and significant up to three disc radii from it in younger and 1 radius in older subjects but was insignificant in abduction.

**CONCLUSIONS.** Horizontal duction compresses the temporal peripapillary choroid, more in adduction than in abduction and more in younger than older subjects. This reflects duction-related peripapillary tissue deformation probably related, at least in part, to optic nerve tethering in adduction.

Keywords: choroid, duction, eye movement, OCT

When the human eye rotates into a large angle adduction, we have shown by magnetic resonance imaging (MRI) that the optic nerve (ON) and its sheath tether the globe and exert tractional force on the optic disc.<sup>1,2</sup> We have also demonstrated by optical coherence tomography (OCT) that adduction deforms the peripapillary Bruch's membrane (ppBM) and tilts the ON head (ONH) anteroposteriorly.<sup>3</sup> The deformation is exaggerated at a threshold of approximately 26° adduction, the angle at which the limited ON length necessitates the onset of tethering.<sup>3,4</sup> Although some reversal of the see-saw tilting of the disc also occurs in abduction, the greater deformation in adduction than abduction is probably due to ON tethering.

Finite element analysis has been used to simulate mechanical stress and strain in the ONH and the peripapillary retina during horizontal eye rotation,<sup>5,6</sup> and we have shown this to be especially the case in adduction.<sup>7</sup> Those simulations suggest that ON tethering force is concentrated on the temporal disc and peripapillary tissue, in the typical location where peripapillary atrophy occurs in patients with primary open angle glaucoma (POAG).<sup>8-10</sup> Simulations further suggest that adduction tethering can deform the optic disc more than extreme, acute intraocular pressure (IOP) elevation, providing

a possible explanation, at least in part, for the many cases of POAG where there is glaucomatous optic neuropathy without abnormally elevated IOP.<sup>11-13</sup> It has been speculated that horizontal eye movements that repetitively deform the optic disc and peripapillary retina may contribute to the peripapillary chorioretinal atrophy common in glaucoma.<sup>10</sup> In addition, choroidal microvascular dropout in regions of peripapillary atrophy occurs in POAG where it is associated with advanced visual field defects.<sup>14</sup>

Our earlier OCT studies showed that horizontal duction deforms ppBM and the superficial ON vasculature.<sup>3,15-17</sup> We have not previously investigated the effect of gaze direction on choroidal volume nor the effect of subject age on such changes. This current study sought evidence of possible deformation of the peripapillary choroid (ppC). The ppC has been reported to thin during both adduction and abduction.<sup>4</sup> We sought to extend the investigation to choroidal volume. Choroidal thinning due to the loss of inner choroidal vessels is linked to POAG<sup>18</sup> and normal tension glaucoma (NTG).<sup>19-21</sup> Older people typically have thinner choroids,<sup>22-26</sup> and thus, choroidal volume and deformation have been proposed to be associated with other age-related ocular diseases.<sup>26</sup> In this study, we examined choroidal deformation in different age groups by



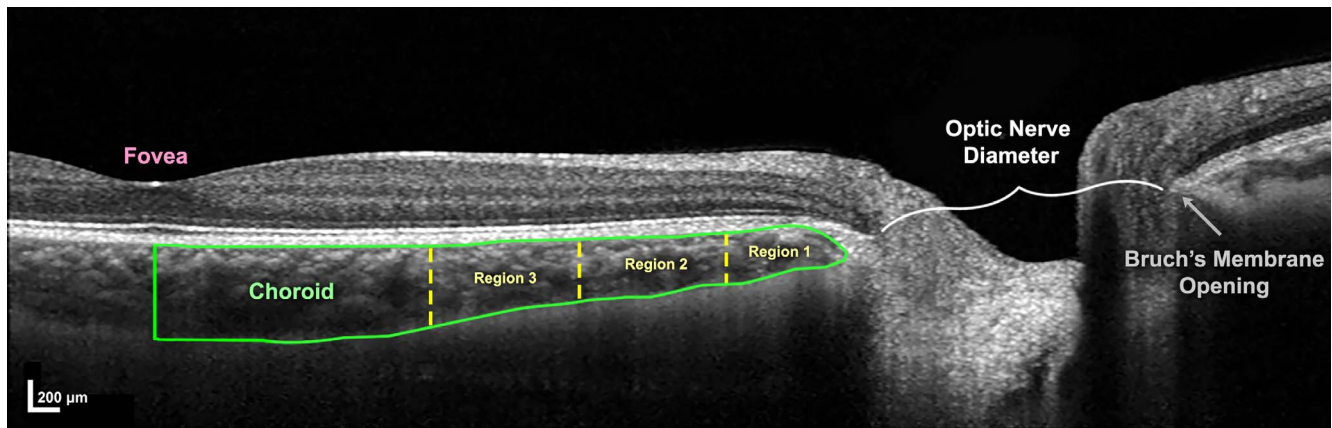


**FIGURE 1.** The choroid was outlined (green) from the temporal edge of Bruch's membrane to the fovea and then separated into three contiguous regions (yellow), each equal to the BMO radius beginning at the temporal margin of the BMO.

quantifying the choroidal volume change resultant from horizontal duction.

## METHODS

### Subjects

Forty volunteers (19 male and 21 female; mean age,  $37 \pm 20$  [standard deviation, SD] years; range, 18–73) were recruited for the study. Subjects, who had not previously participated in research of this sort, were separated into a younger group of 25 (15 male and 10 female; mean age,  $24 \pm 5$ ; range, 18–33) and an older group of 15 volunteers (4 male and 11 female; mean age,  $62 \pm 8$  years; range, 50–73). Subjects gave written informed consent before participating according to a protocol approved by the University of California, Los Angeles, Institutional Review Board and compliant with the Declaration of Helsinki. Ophthalmic evaluations were performed of all subjects to confirm normal corrected visual acuity and absence of any ocular abnormalities besides refractive error and pseudophakia. Subjects had normal IOP ( $<21$  mm Hg), normal binocular alignment, and normal ONs. The mean spherical equivalent refractive error where determined was  $-1.5 \pm 2.9$  (SD; range, +2 to  $-8.3$ ), although refractive error was not ascertained for 24 volunteers.

### Optical Coherence Tomography

A spectral domain OCT scanner (Spectralis; Heidelberg Engineering, Heidelberg, Germany) was used to image the choroid with enhanced depth imaging. Volume scans of both eyes in central gaze, abduction ( $35^\circ$ ), and adduction ( $35^\circ$ ) were performed sequentially. Imaging consisted of 25 horizontal B-scans covering a  $30^\circ \times 5^\circ$  rectangular region centered between the fovea and disc at vertical increments of approximately  $62 \mu\text{m}$ , depending on the focal depth. To scan in the eccentric gazes, the OCT imager was pivoted in yaw to angles set by goniometric scale placed on the instrument's gimbal. For standardization, the raster was rotated for every scan to align the center of the disc with the fovea. This rotation compensated for ocular torsion, which according to Listing's Law varies systematically with gaze direction, but typically by different amounts in each eye of the same individual, and differently among individuals.<sup>27,28</sup> Torsional correction of the OCT scan raster, thus, cancelled the effect of ocular torsion and rendered otherwise superimposable the sets of images obtained in multiple gaze positions.

Axial tilt of the B-scans was maintained because the scanning light beam always entered the eye at the same angle relative to the visual direction. The axial tilt of the B-scans was held constant because when the scanner head rotated, the eye rotated with it maintain fixation on the scanner's internal target. Thus, the angle of beam entrance into the eye did not change with gaze direction. Subjects' heads were fixed straight ahead with straps and cushions. Subjects were instructed to maintain this head position as they fixated the scanner's internal target that was measured to be offset  $12^\circ$  nasally from straight ahead.<sup>3</sup> Rotation of the OCT imager was mechanically limited to  $35^\circ$  by its design.

### Image Analysis

Images were processed with Adobe Photoshop (Adobe Systems, San Jose, CA, USA) as TIFF files. The scans were cropped, scaled, and, if necessary, rotated to correct the aspect ratio so that peripheral retinal features were in precise alignment for all gaze positions for the same eye. Images were converted to a volumetric stack in Materialise Mimics (Materialise, Leuven, Flemish Brabant, Belgium) with the slices in original scaling ( $3.87 \mu\text{m}/\text{pixel}$  horizontally, an average of  $11.6 \mu\text{m}/\text{pixel}$  in depth, and an average of  $62.1 \mu\text{m}/\text{slice}$  vertically [distance between B-scans]). For each stack, the middle 12 slices of the 25 acquired were all analyzed in order to evaluate the ppC, as these 12 slices consistently straddled the central optic disc. Tracing of the choroid was temporally bounded nasally by the Bruch's membrane opening (BMO). The ppC was then segmented into three contiguous regions with horizontal dimensions equal to the BMO radius, beginning at the temporal edge of the BMO (Fig. 1). For each eye in each subject, a three-dimensional representation of the temporal ppC was rendered from 12 traced cross-sections, with the distance between B-scans as the interval with which the summed areas were multiplied to generate the volume. Each eye was treated as a separate sample in the analyses.

We analyzed two parameters for the scans in each eccentric gaze relative to central gaze: (1) change in volume of the choroid within the three total regions, and (2) variation among the three segmented regions. These changes were then compared between younger and older age groups.

### Statistical Analysis

In order to account for possible interocular correlation between the two eyes of the same subject and among choroidal regions in the same eye, statistical analysis was

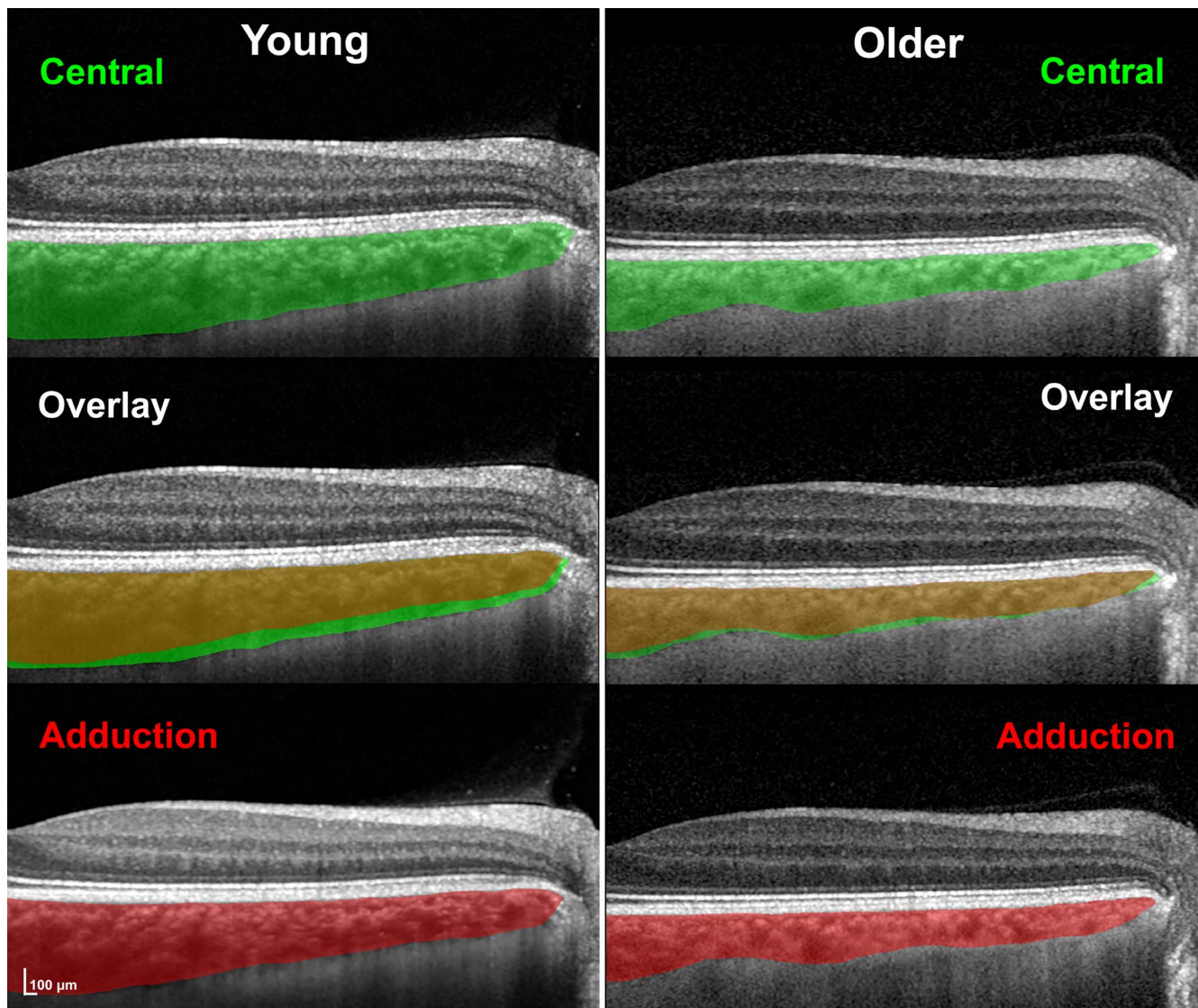


**FIGURE 2.** Optical coherence tomography of choroid between temporal edge of optic disc (*right*) and foveola (*left*) color in a young (*left* column) and an older subject (*right* column). *Top* row: central gaze. *Bottom* row: adduction. The central row overlays images in central gaze and adduction so that overlapping choroidal regions appear *yellow-brown* but areas of choroidal thinning in adduction appear *green*. Note greater choroidal thinning in adduction in the young subject.

executed utilizing generalized estimating equations (GEE) with SPSS software (version 24.0; IBM Corp., Armonk, NY, USA), with eye and choroidal region as nested, within-subject variables. The statistical package reports significant values to only three decimal places based upon a  $\chi^2$  distribution, but this is not a simple  $\chi^2$  test of simple proportions. Where the SPSS package reported significance at  $P=0.000$ , we also note the  $\chi^2$  value and number of degrees of freedom for the reader's interest because probabilities of the random significant differences for the findings reported here could never be exactly zero.

## RESULTS

### Choroidal Volume in Younger and Older Subjects

Images in Figure 2 illustrate the decrease in choroid volume reduction when gaze shifts from central to adduction in example and younger and older subjects. The choroid typically

appeared thicker in younger than older subjects, with supported measurements showing  $556 \pm 25$  nanoliters (nL) (standard error of the mean) average choroidal volume in central gaze in younger subjects but only  $460 \pm 21$  nL in older subjects ( $P < 0.01$ ). Choroidal volume was also greater in younger than older subjects in eccentric horizontal gazes but was always less in adduction than in central gaze in both groups. In adduction, choroidal volume in younger subjects decreased to  $514 \pm 24$  nL but in older subjects decreased less so to  $454 \pm 21$  nL, reducing to statistical insignificance the difference between groups. In adduction, choroidal volume of younger subjects increased insignificantly to  $559 \pm 26$  nL and that of the older group remained  $460 \pm 21$  nL so that the difference between groups again became significant ( $P < 0.01$ ).

### Test-Retest Variability

Test-retest variability was evaluated by repeating the experiment on different days in 10 eyes of 5 young subjects by using

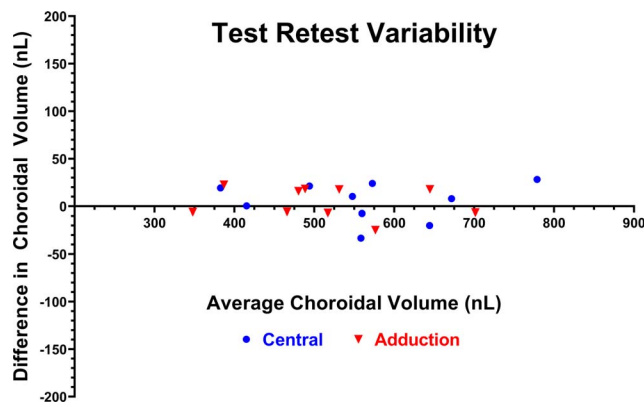


FIGURE 3. Bland-Altman plot of test-retest variability in 10 eyes of 5 young subjects who were each tested twice in both central gaze and adduction.

identical data collection and analysis to compute choroidal volume in both central gaze and adduction. As shown in Figure 3, Bland-Altman analysis of test-retest agreement was performed, demonstrating for central gaze a mean choroidal volume of 562 nL, with bias of 5 nL ( $<0.9\%$ ) in the repeat measurement relative to the first measurement. For central gaze, the 95% limits of agreement were from  $-34$  to 45 nL, representing a maximum 8% for individual measurements. In adduction, the comparable values were 514 nL, with bias of 4 nL ( $<0.8\%$ ). The 95% limits of agreement were from  $-27$  to 36 nL, representing a maximum 7% for individual measurements. This implies that test-retest variability would account for no more than 0.9% difference in average measurements. The first and second sets of measurements in each eye, in both central gaze and adduction, were also compared using linear regression for difference from the null hypothesis of unity slope, the ideal value if both sets of measurements were identical in every eye. For both primary gaze and adduction choroidal volumes, neither regression slope differed significantly from unity ( $P > 0.75$ ), indicating that the repeat experiments yielded statistically similar results to the initial experiments.

### Change in Choroidal Volume with Gaze

Choroidal volume change from central gaze was significantly related to gaze position as a factor ( $P = 0.000$ , GEE  $\chi^2 = 47$ , 2 degrees of freedom [df]). In both younger (Fig. 2) and older subjects, choroidal volume consistently decreased in adduction but did not change much in abduction (Fig. 4). In younger subjects, mean choroidal volume decreased in adduction by  $42 \pm 3$  nL ( $P < 0.0001$ ), a value about 8-fold greater than test-retest variability. Choroidal volume insignificantly increased by  $2 \pm 3$  nL in abduction. In older subjects, choroidal volume decreased by  $6 \pm 3$  nL in adduction ( $P < 0.02$ ) and increased insignificantly by  $1 \pm 4$  nL in abduction. There was a significant interaction of gaze position with age ( $P = 0.000$ , GEE  $\chi^2 = 17$ , 2 df).

It is informative to evaluate the change in choroidal volume relative to central gaze. In the younger subjects, adduction was associated with a  $7.5\% \pm 0.6\%$  mean decrease in choroidal volume ( $P < 0.001$ ), whereas in abduction, there was an insignificant  $0.4\% \pm 0.4\%$  increase in volume. In the older subjects, adduction was associated with a  $1.3\% \pm 0.6\%$  mean decrease in choroidal volume ( $P < 0.02$ ), whereas in abduction there was an insignificant  $0.2\% \pm 0.7\%$  increase in volume.

In younger subjects, relative choroidal volume change in adduction was greatest in the immediate peripapillary zone

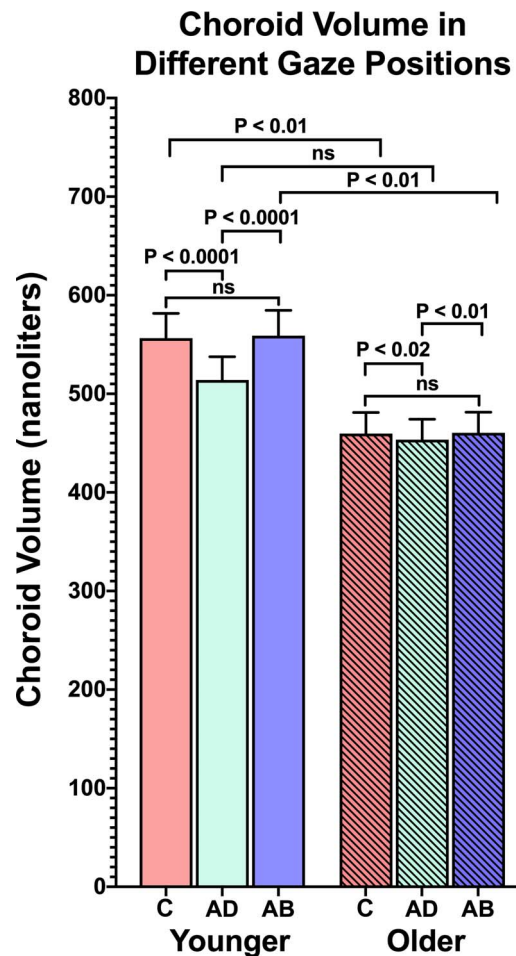


FIGURE 4. Temporal peripapillary choroidal volume in central gaze, adduction, and abduction for younger and older subjects. Choroidal volume was less in adduction than in central gaze in both younger and older subjects but did not change in abduction. C, central gaze; AD, adduction; AB, abduction. Solid-colored bars indicate data of 50 eyes of younger subjects. Hatched bars indicate data of 30 eyes of older subjects. 95% confidence limits.

and decreased progressively with distance from the disc margin ( $\chi^2 = 19$ ). As shown in Figure 5, in younger subjects during adduction, choroidal volume within one radius of the disc decreased  $12\% \pm 1\%$ , between one and two radii decreased  $2\% \pm 1\%$ , and between two and three radii decreased  $1\% \pm 1\%$ . In these younger subjects, the relative volume decrease in abduction was significant only within one disc radius of the disc margin (1 disc radius [R];  $P < 0.01$ ). In older subjects, relative choroidal volume did not change significantly in adduction or abduction in any region.

### DISCUSSION

Previous studies have shown that horizontal duction, particularly adduction, deforms the optic disc and surrounding peripapillary tissues.<sup>4,15-17</sup> This deformation in adduction includes temporal shifting of the nasal part of the disc, anteroposterior displacement of the ppBM, and tilting of the disc. The current study demonstrates that temporal ppC volume decreases more in adduction than in abduction, extending prior findings that adduction deforms the peripapillary retina. Most of the compression of the temporal choroid during horizontal duction occurs near the disc, suggesting that

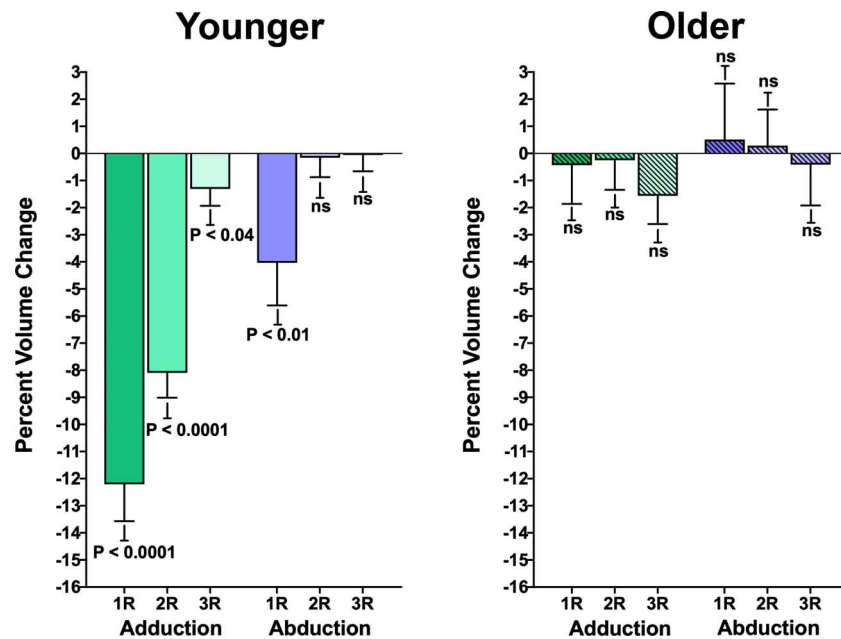


FIGURE 5. Volume change in the temporal papillary choroid, relative to central gaze, was greater in regions nearest the optic disc in younger subjects. Data are from 50 eyes of younger and 30 eyes of older subjects. Brackets mark 95% confidence intervals. R, disc radius, as defined in the text.

the deformation is due to force transmission by the ON or its sheath during eye movements.

Compression of the temporal choroid is associated with deformation of the peripapillary retina and ON fibers. The temporal choroid is compressed during adduction in both younger and older subjects but approximately 15-fold more so in adduction than in abduction in younger subjects. This greater compression in adduction than abduction is consistent with optical imaging showing greater deformation of the disc and peripapillary retina in these duction directions<sup>15</sup> and the observation by MRI imaging of ON tethering only in adduction.<sup>3,4,29</sup> Compression of the temporal choroid is also consistent with observed temporal displacement of peripapillary vessels<sup>15</sup> and the overall temporalward compression of optic disc tissue during ON tethering in adduction.<sup>2</sup> The situation in abduction is quite different, being associated with only minimal choroidal compression and less ON and peripapillary deformations in young adults but none in older subjects.<sup>15</sup> This difference between adduction and abduction is also consistent with MRI studies showing that the ON is usually slack during abduction.<sup>2</sup>

In general, younger people may have more compliant peripapillary tissues than older people because of age-related stiffening in sclera,<sup>30-32</sup> Bruch's membrane,<sup>33</sup> and lamina cribrosa.<sup>34-37</sup> As such, ppC deformation would be expected to be less in older people who have stiffer tissues surrounding the choroid. Older people generally have thinner choroids,<sup>22-26</sup> perhaps accounting for the relatively smaller change in choroidal volume in the eccentric gaze positions in older people. Subjects with NTG have significantly thinner choroids than normal in the inferonasal, inferior, and inferotemporal regions.<sup>18</sup> Choroids of subjects with both NTG and high myopia average significantly thinner than normal at the fovea, superior, superotemporal, temporal, and inferotemporal regions than at the ONH.<sup>21</sup> In light of the correlation between decreasing choroidal thickness and age-related ocular neuropathies, choroidal thinning might be a cause or effect of glaucomatous optic neuropathy because choroidal thickness is

subnormal in both ordinary NTG<sup>20,38,39</sup> and highly myopic NTG.<sup>21</sup>

During adduction, the disc and the peripapillary retina shift and tilt, signifying that this entire region undergoes mechanical strain. Some of the blood supply to the ON arises from the choroid.<sup>40-42</sup> Compression of the ppC in adduction might interfere with some of the blood supply to the ON,<sup>40</sup> which may eventually damage these tissues in situations where there is also compromise to the posterior ciliary circulation. Choroidal vascular insufficiency might, thus, contribute to optic neuropathies, such as glaucoma.<sup>41,42</sup> There are conflicting reports regarding the relationship between choroidal thickness and glaucoma, with some histologic and in vivo studies showing a thinner ppC in glaucomatous eyes,<sup>18,19,43</sup> but other studies finding no association.<sup>44-49</sup> However, the present study provides in vivo evidence that adduction instantaneously compresses the ppC. As this study only includes healthy subjects, future research could investigate possible gaze-evoked changes in the choroidal volume of patients with glaucoma to clarify a possible relationship between choroidal deformation and glaucoma.

There may be pathologic implication to the lesser choroidal compression in adduction observed here in older than younger subjects. This might be the consequence of remodeling induced by the accumulation of strains during adduction eye movements. The thinner elderly choroids are probably also sclerotic, containing proportionately more rigid connective tissue than younger choroids. If so, choroidal volume reduction in adduction would be diminished by greater resistance to mechanical strain imposed by the tethering ON. Our MRI studies have demonstrated that the ON becomes tethered when adduction exceeds 26° in people of all ages<sup>3,4</sup> so that reaction force to the powerful medial rectus muscle must, in everyone, deform or displace the globe to permit further adduction. Limited ON length makes local deformation in the eye or orbit geometrically inevitable. Healthy deformation—"strain" in mechanical terminology—would ideally occur only in compliant tissues that are not functionally compromised by deformation and so dissipate

the mechanical force harmlessly. We propose that the choroid is among the tissues that safely absorb mechanical strain during adduction. Choroidal deformation normally acts like a cushion to avert the transfer of mechanical strain to critical tissues, such as the lamina cribrosa and ON. Sclerosis of the choroid and other peripapillary tissues would defeat the cushioning function and transfer potentially damaging strain to critical tissues, such as the ON. A relatively thin and poorly compressible ppC would then be a pathogenic factor in optic neuropathy, including glaucoma.

This study was limited to imaging of the temporal peripapillary region. Although more remote areas of the choroid could not be evaluated, absence of significant eye movement-related changes in choroidal volume beyond three disc radii from the border of the BMO is highly suggestive that the effects of eye movement are limited to this region, but the current study cannot verify this directly. This study did not include graded duction angles and, thus, cannot determine if a threshold exists for gaze-evoked choroidal deformation, as has been shown in Bruch's membrane deformation.<sup>3</sup> The current study did not measure choroidal blood flow.

### Acknowledgments

Disclosure: **J.Y. Chen**, None; **A. Le**, None; **L.M. De Andrade**, None; **T. Goseki**, None; **J.L. Demer**, None

### References

- Demer JL, Clark RA, Suh SY, et al. Magnetic resonance imaging of optic nerve traction during adduction in primary open-angle glaucoma with normal intraocular pressure. *Invest Ophthalmol Vis Sci*. 2017;58:4114-4125.
- Demer JL. Optic nerve sheath as a novel mechanical load on the globe in ocular duction. *Invest Ophthalmol Vis Sci*. 2016; 57:1826-1838.
- Suh SY, Le A, Shin A, Park J, Demer JL. Progressive deformation of the optic nerve head and peripapillary structures by graded horizontal duction. *Invest Ophthalmol Vis Sci*. 2017;58:5015-5021.
- Chang MY, Shin A, Park J, et al. Deformation of optic nerve head and peripapillary tissues by horizontal duction. *Am J Ophthalmol*. 2017;174:85-94.
- Wang X, Rumpel H, Lim WE, et al. Finite element analysis predicts large optic nerve head strains during horizontal eye movements. *Invest Ophthalmol Vis Sci*. 2016;57:2452-2462.
- Wang X, Fisher LK, Milea D, Jonas JB, Girard MJ. Predictions of optic nerve traction forces and peripapillary tissue stresses following horizontal eye movements. *Invest Ophthalmol Vis Sci*. 2017;58:2044-2053.
- Shin A, Yoo L, Park J, Demer JL. Finite element biomechanics of optic nerve sheath traction in adduction. *J Biomech Eng*. 2017;139.
- Uchida H, Ugurlu S, Caprioli J. Increasing peripapillary atrophy is associated with progressive glaucoma. *Ophthalmology*. 1998;105:1541-1545.
- Park KH, Tomita G, Liou SY, Kitazawa Y. Correlation between peripapillary atrophy and optic nerve damage in normal-tension glaucoma. *Ophthalmology*. 1996;103:1899-1906.
- Jonas JB. Clinical implications of peripapillary atrophy in glaucoma. *Curr Opin Ophthalmol*. 2005;16:84-88.
- Zhao J, Solano MM, Oldenburg CE, et al. Prevalence of normal-tension glaucoma in the chinese population: A systematic review and meta-analysis. *Am J Ophthalmol*. 2019;199:101-110.
- Iwase A, Suzuki Y, Araie M, et al. The prevalence of primary open-angle glaucoma in japanese: the Tajimi study. *Ophthalmology*. 2004;111:1641-1648.
- Kim JH, Kang SY, Kim NR, et al. Prevalence and characteristics of glaucoma among Korean adults. *Korean J Ophthalmol*. 2011;25:110-115.
- Rao HL, Sreenivasaiah S, Riyazuddin M, et al. Choroidal microvascular dropout in primary angle closure glaucoma. *Am J Ophthalmol*. 2019;199:184-192.
- Le A, Chen J, Lesgart M, Gawargious BA, Suh SY, Demer JL. Age-dependent deformation of the optic nerve head and peripapillary retina by horizontal duction. *Am J Ophthalmol*. In press.
- Sibony PA. Gaze evoked deformations of the peripapillary retina in papilledema and ischemic optic neuropathy. *Invest Ophthalmol Vis Sci*. 2016;57:4979-4987.
- Wang X, Beotra MR, Tun TA, et al. In vivo 3-dimensional strain mapping confirms large optic nerve head deformations following horizontal eye movements. *Invest Ophthalmol Vis Sci*. 2016;57:5825-5833.
- Yin ZQ, Vaegan, Millar TJ, Beaumont P, Sarks S. Widespread choroidal insufficiency in primary open-angle glaucoma. *J Glaucoma*. 1997;6:23-32.
- Park HY, Lee NY, Shin HY, Park CK. Analysis of macular and peripapillary choroidal thickness in glaucoma patients by enhanced depth imaging optical coherence tomography. *J Glaucoma*. 2014;23:225-231.
- Hirooka K, Tenkumo K, Fujiwara A, Baba T, Sato S, Shiraga F. Evaluation of peripapillary choroidal thickness in patients with normal-tension glaucoma. *BMC Ophthalmol*. 2012;12: 29.
- Usui S, Ikuno Y, Miki A, Matsushita K, Yasuno Y, Nishida K. Evaluation of the choroidal thickness using high-penetration optical coherence tomography with long wavelength in highly myopic normal-tension glaucoma. *Am J Ophthalmol*. 2012;153:10-16.
- Rhodes LA, Huisingh C, Johnstone J, et al. Peripapillary choroidal thickness variation with age and race in normal eyes. *Invest Ophthalmol Vis Sci*. 2015;56:1872-1879.
- Huang W, Wang W, Zhou M, et al. Peripapillary choroidal thickness in healthy chinese subjects. *BMC Ophthalmol*. 2013;13:23.
- Johnstone J, Fazio M, Rojananuangnit K, et al. Variation of the axial location of Bruch's membrane opening with age, choroidal thickness, and race. *Invest Ophthalmol Vis Sci*. 2014;55:2004-2009.
- Huang W, Wang W, Gao X, et al. Choroidal thickness in the subtypes of angle closure: an EDI-OCT study. *Invest Ophthalmol Vis Sci*. 2013;54:7849-7853.
- Margolis R, Spaide RF. A pilot study of enhanced depth imaging optical coherence tomography of the choroid in normal eyes. *Am J Ophthalmol*. 2009;147:811-815.
- Demer JL. Pivotal role of orbital connective tissues in binocular alignment and strabismus: the friedenwald lecture. *Invest Ophthalmol Vis Sci*. 2004;45:729-738.
- Demer JL. Current concepts of mechanical and neural factors in ocular motility. *Curr Opin Neurol*. 2006;19:4-13.
- Suh SY, Clark RA, Demer JL. Optic nerve sheath tethering in adduction occurs in esotropia and hypertropia, but not in exotropia. *Invest Ophthalmol Vis Sci*. 2018;59:2899-2904.
- Geraghty B, Jones SW, Rama P, Akhtar R, Elsheikh A. Age-related variations in the biomechanical properties of human sclera. *J Mech Behav Biomed Mater*. 2012;16:181-191.
- Coudrillier B, Tian J, Alexander S, Myers KM, Quigley HA, Nguyen TD. Biomechanics of the human posterior sclera: Age- and glaucoma-related changes measured using inflation testing. *Invest Ophthalmol Vis Sci*. 2012;53:1714-1728.
- Avetisov ES, Savitskaya NF, Vinetskaya MI, Iomdina EN. A study of biochemical and biomechanical qualities of normal and myopic eye sclera in humans of different age groups. *Metab Pediatr Syst Ophthalmol*. 1983;7:183-188.

33. Booi J, Baas DC, Beisekeeva J, Gorgels TG, Bergen AA. The dynamic nature of Bruch's membrane. *Prog Retin Eye Res.* 2010;29:1-18.
34. Albon J, Karwatowski WS, Easty DL, Sims TJ, Duance VC. Age related changes in the non-collagenous components of the extracellular matrix of the human lamina cribrosa. *Br J Ophthalmol.* 2000;84:311-317.
35. Albon J, Karwatowski WS, Avery N, Easty DL, Duance VC. Changes in the collagenous matrix of the aging human lamina cribrosa. *Br J Ophthalmol.* 1995;79:368-375.
36. Albon J, Purslow PP, Karwatowski WS, Easty DL. Age related compliance of the lamina cribrosa in human eyes. *Br J Ophthalmol.* 2000;84:318-323.
37. Leung LK, Ko MW, Lam DC. Effect of age-stiffening tissues and intraocular pressure on optic nerve damages. *Mol Cell Biomech.* 2012;9:157-173.
38. Hirooka K, Fujiwara A, Shiragami C, Baba T, Shiraga F. Relationship between progression of visual field damage and choroidal thickness in eyes with normal-tension glaucoma. *Clin Exp Ophthalmol.* 2012;40:576-582.
39. Park JH, Yoo C, Kim YY. Peripapillary choroidal thickness in untreated normal-tension glaucoma eyes with a single-hemifield retinal nerve fiber layer defect. *Medicine (Baltimore).* 2018;97:e11001.
40. Hayreh SS. The blood supply of the optic nerve head and the evaluation of it—myth and reality. *Prog Retin Eye Res.* 2001;20:563-593.
41. Hayreh SS. Blood supply of the optic nerve head and its role in optic atrophy, glaucoma, and oedema of the optic disc. *Br J Ophthalmol.* 1969;53:721-748.
42. Hayreh SS, Revie IH, Edwards J. Vasogenic origin of visual field defects and optic nerve changes in glaucoma. *Br J Ophthalmol.* 1970;54:461-472.
43. Kubota T, Jonas JB, Naumann GO. Decreased choroidal thickness in eyes with secondary angle closure glaucoma. An aetiological factor for deep retinal changes in glaucoma? *Br J Ophthalmol.* 1993;77:430-432.
44. Ehrlich JR, Peterson J, Parlitsis G, Kay KY, Kiss S, Radcliffe NM. Peripapillary choroidal thickness in glaucoma measured with optical coherence tomography. *Exp Eye Res.* 2011;92:189-194.
45. Li L, Bian A, Zhou Q, Mao J. Peripapillary choroidal thickness in both eyes of glaucoma patients with unilateral visual field loss. *Am J Ophthalmol.* 2013;156:1277-1284.
46. Mwanza JC, Hochberg JT, Banitt MR, Feuer WJ, Budenz DL. Lack of association between glaucoma and macular choroidal thickness measured with enhanced depth-imaging optical coherence tomography. *Invest Ophthalmol Vis Sci.* 2011;52:3430-3435.
47. Suh W, Cho HK, Kee C. Evaluation of peripapillary choroidal thickness in unilateral normal-tension glaucoma. *Jpn J Ophthalmol.* 2014;58:62-67.
48. Maul EA, Friedman DS, Chang DS, et al. Choroidal thickness measured by spectral domain optical coherence tomography: factors affecting thickness in glaucoma patients. *Ophthalmology.* 2011;118:1571-1579.
49. Lee S, Han SX, Young M, Beg MF, Sarunic MV, Mackenzie PJ. Optic nerve head and peripapillary morphometrics in myopic glaucoma. *Invest Ophthalmol Vis Sci.* 2014;55:4378-4393.